Absolute atomic hydrogen densities in a radio frequency discharge measured by two-photon laser induced fluorescence imaging

Laurence Chérigier-Kovacic, U Czarnetzki, D Luggenhölscher, V Schulz-von Der Gathen, H F Döbele

Absolute atomic hydrogen densities in a radio frequency discharge measured by two-photon laser induced fluorescence imaging

L. Chérigier, U. Czarnetzki, D. Luggenhölscher, V. Schulz-von der Gathen, and H. F. Döbele

Citation: Journal of Applied Physics **85**, 696 (1999); doi: 10.1063/1.369149
View online: http://dx.doi.org/10.1063/1.369149
View Table of Contents: http://scitation.aip.org/content/aip/journal/jap/85/2?ver=pdfcov
Published by the AIP Publishing

Absolute atomic hydrogen densities in a radio frequency discharge measured by two-photon laser induced fluorescence imaging

L. Chérigier,[a] U. Czarnetzki,[b] D. Luggenhölscher, V. Schulz-von der Gathen, and H. F. Döbele
Institut für Laser- und Plasmaphysik, Universität GH Essen, 45117 Essen, Germany

(Received 13 July 1998; accepted for publication 16 October 1998)

Absolute atomic hydrogen densities were measured in the gaseous electronics conference reference cell parallel plate reactor by Doppler-free two-photon absorption laser induced fluorescence spectroscopy (TALIF) at $\lambda=205$ nm. The capacitively coupled radio frequency discharge was operated at 13.56 MHz in pure hydrogen under various input power and pressure conditions. The Doppler-free excitation technique with an unfocused laser beam together with imaging the fluorescence radiation by an intensified charge coupled device camera allows instantaneous spatial resolution along the radial direction. Absolute density calibration is obtained with the aid of a flow tube reactor and titration with NO_2. The influence of spatial intensity inhomogenities along the laser beam and subsequent fluorescence are corrected by TALIF in xenon. A full mapping of the absolute density distribution between the electrodes was obtained. The detection limit for atomic hydrogen amounts to about 2×10^{18} m^{-3}. The dissociation degree is of the order of a few percent. © *1999 American Institute of Physics.* [S0021-8979(99)05602-9]

I. INTRODUCTION

Radio frequency (rf) discharges are widely used in technical plasma processes like thin-film deposition and etching. They represent a major topic in present day low temperature plasma research.[1–4] Hydrogen plays a key role in many technical discharges.[5,6] The precise determination of the absolute density distribution is important for understanding both the discharge mechanism and the plasma-induced processes. Spatially resolved atomic hydrogen density measurements are therefore the aim of this study.

Laser induced fluorescence spectroscopy has long been proved to be a sensitive and nonperturbing tool for the detection of low concentrations of atoms and molecules.[7] In atomic hydrogen, the excitation wavelength to the lowest excited state is at $\lambda=121.6$ nm—difficult to generate and strongly absorbed in air or other gases. In addition, the fluorescence light is emitted at the same wavelength and self-absorption occurs. Two-photon excitation can overcome these problems. Various alternative excitation schemes have been proposed.[8] With excitation at $\lambda=205$ nm to $n=3$, fluorescence light in the visible at Balmer α ($\lambda=656$ nm) can be observed.

This scheme has been successfully applied to a number of discharges and flames.[9,10] However, since the excitation efficiency of a two-photon step is smaller by many orders of magnitude as compared to single-photon resonances a focused laser beam is usually used, and fluorescence signals originate at the focal region only. For spatially resolved measurements, therefore, data acquisition has to be performed point by point, and the laser beam together with the detection optics have to be moved with respect to the discharge chamber. Doppler-free excitation can greatly improve the efficiency, provided the laser bandwidth (0.14 cm^{-1} in our case) is significantly smaller than the Doppler width (1.2 cm^{-1} at 300 K). In this case an unfocused laser beam can be used with the advantage of inherent spatial resolution along the beam.

This technique is demonstrated in this article in connection with the determination of the spatial distribution of the absolute atomic hydrogen density in the gaseous electronics conference (GEC) reference cell parallel plate reactor. In addition, a novel calibration technique by xenon is presented. In connection with these measurements the energy of a xenon Rydberg state, the natural lifetime of this state, and the self-quenching coefficient have been determined.

The article is organized as follows: First we describe briefly the experimental setup, then calibration measurements both in xenon and with the aid of a flow tube reactor. In the main part of the article the experimental results in the hydrogen rf discharge are shown. Finally the results are summarized.

II. EXPERIMENTAL SETUP

The experimental setup is shown in Fig. 1. The GEC reference cell is described in detail elsewhere.[11,12] In brief, it is a capacitively coupled rf reactor with two parallel water cooled aluminum electrodes of 10 cm diam and a discharge gap of 2.5 cm. Each electrode is surrounded by a grounded cylinder, the so-called ''guard rings.'' The upper electrode serves also as the gas supply and has a large number of small holes: a so-called ''showerhead'' electrode. The discharge is operated in pure hydrogen at pressures between 25 and 85 Pa and rf powers between 20 and 100 W (difference between

[a]Present address: Equipe Turbulence Plasma, UMR 6633, Université de St. Jérôme, Avenue Escadrille Normandie-Niemen, 13397 Marseille, France.
[b]Author to whom correspondence should be addressed; electronic mail: uwe.czarnetzki@uni-essen.de

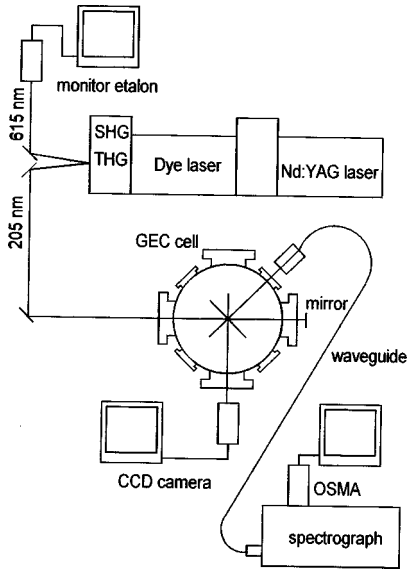

FIG. 1. Experimental setup (SHG: second harmonic generation, THG: third harmonic generation, OSMA: optical spectroscopic multichannel analyzer).

forward and reflected power), corresponding to peak-to-peak voltages between 600 and 800 V and bias voltages between 210 and 370 V, respectively. The flow rate is between 30 and 80 sccm, depending on pressure. The upper electrode, the showerhead, is powered in the present case; the lower electrode is grounded. The rf voltage is supplied to the electrodes by an automatic matching unit. Electrode voltages are measured by a high voltage probe (Tektronix P6015A) in combination with a fast digital storage oscilloscope.

The exciting radiation at $\lambda=205$ nm is generated by a Nd:YAG-pumped dye laser (Continuum Powerlite 8010 and ND6000) with a fixed frequency of 10 Hz radiating at $\lambda=615$ nm with subsequent frequency doubling in KDP and mixing in BBO. About 3 mJ in 3 ns pulses at a bandwidth of 0.14 cm^{-1} are obtained. The beam diameter is about 5 mm. The laser beam passes through the radial center of the discharge, and Doppler-free excitation is realized by a mirror close to the exit window that reflects the laser beam back into itself. The precise overlap of the two beams is checked at a distance of 3 m; the alignment error is less than 1 mrad. The beam diameter is too small to allow a complete mapping of the axial dimension within one measurement. In consecutive measurements the laser beam is therefore aligned at 15 equally spaced axial positions ($\Delta z=1.5$ mm) in order to cover the entire region between the electrodes.

Fluorescence light at $\lambda=656$ nm is imaged perpendicular to the laser beam onto a gated intensified charge coupled device (ICCD) camera (Princeton Instruments) with an edge filter ($\lambda_0=645$ nm) in front. Imaging is by a lens system with an open aperture of 2 cm placed 30 cm from the center of the discharge. The demagnification factor is 2.3. The gate width is 20 ns, and light from several laser shots (typical 150) is accumulated on the camera before readout. The imaging covers the area from the radial center of the electrodes to the edge.

The magnification factor and the positions of the electrodes are determined by a calibration measurement. In a plastic block optical fibers of 100 μm diam are fixed at six different positions. This block is placed on the lower electrode with the fiber ends located at the plane of laser beam. The fibers are illuminated and from the image on the ICCD camera the magnification factor and the absolute positions in the radial and axial directions result.

Light from the center of the discharge is imaged by a second lens ($f=80$ cm) with an aperture of 13 mm onto a 100 μm quartz fiber connected to a 2 m Czerny–Turner spectrograph (Jarrell Ash) equipped with an intensified diode array (Princeton Instruments). This allows us to detect plasma-induced emission from atoms and molecules. The optical fiber can be moved along the axial direction of the discharge so that the emission can be scanned over the region from the powered to the grounded electrode. The spatial resolution is difficult to define since light is integrated over the cone imaged onto the fiber. An estimate shows that it is better than 2 mm in our case.

III. CALIBRATION PROCEDURE

A. Relative density calibration by xenon

The generation and the detection of fluorescence light does not take place in a homogenous manner along the radial direction: The excitation rate is not homogeneous due to the divergence of the laser beam, and fluorescence light is collected with different solid angles from the imaged area. These inhomogenities can be corrected in the following way: The GEC cell is filled with xenon without running a discharge. A fluorescence signal is then generated by two-photon absorption. Since the particle density is homogeneous all inhomogenities measured under these conditions are caused by the imaging and the divergence of the laser beam. The measured profile in xenon therefore yields the spatial correction function for the hydrogen measurements.

Xenon has a two-photon resonance between the ground state and the $15p[2\ 1/2](J=2)$ Rydberg state at $\lambda=206$ nm. We did not find the exact value of that resonance in the literature. We therefore determined the absolute value experimentally by measuring the relative shift with respect to the well known value of the hydrogen resonance. Our result for the $15p[2\ 1/2](J=2)$ in xenon is $E=96\,948.2$ cm^{-1}. This is 51.0 cm^{-1} below the $J=3$ state listed in Ref. 13. Several cascading emission channels are possible with the strongest emission around $\lambda=582$ nm to the $5d$ states. In order to suppress stray light from the windows, an edge filter at 570 nm is attached in front of the detector.

The lifetime of the excited state and the self-quenching coefficient were also determined. First, it was verified that the fluorescence signal scales with the square of the laser intensity and that saturation effects by depletion of the ground state population or by ionization are negligible. Then, at a constant pressure of $p_0=4$ Pa, the fluorescence signal S was measured as a function of the gate width of the ICCD camera t_g (Fig. 2). These data are fitted to the theoretical time dependence

$$S=A[1-\exp(-t_g/\tau_0)] \tag{1}$$

with

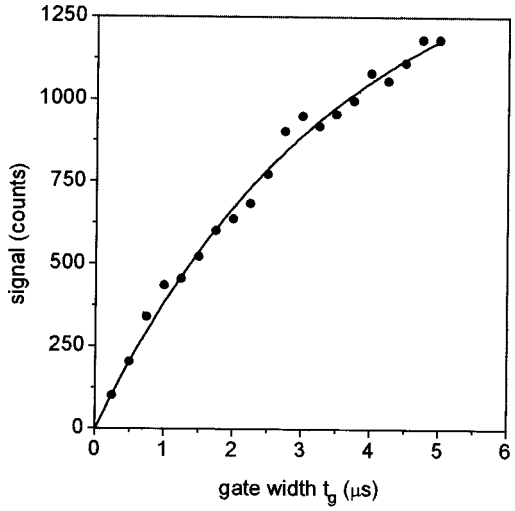

FIG. 2. Fluorescence signal from xenon after two-photon excitation as a function of the gate time of the ICCD camera. Pressure is fixed at $p_0 = 4$ Pa. The solid line is a fit according to Eq. (1).

$$\tau_0 = \tau \Big/ \left(1 + \frac{\tau k_Q}{k_B T_{\mathrm{Xe}}}\, p_0\right). \tag{2}$$

Here, A is an amplitude factor, τ_0 the lifetime at the pressure p_0, τ the natural lifetime of the upper xenon state, k_Q the self-quenching coefficient, k_B the Boltzmann constant, and T_{Xe} the gas temperature. The lifetime obtained from the fit is $\tau_0 = 3.5 \pm 0.3$ μs. In a second measurement the gatewidth was kept constant at $t_g = 5$ μs and the pressure p was varied (Fig. 3). Within this period excited atoms can fly due to their thermal velocities a distance of about 1 mm. Light is collected therefore from a region (8 mm) significantly larger than the laser beam diameter (5 mm) in order to avoid the loss of excited atoms from the detection volume. In the fitted theoretical profile the lifetime τ has been replaced according to Eq. (2) so that, except for an amplitude factor B, only one adjustable parameter α remains

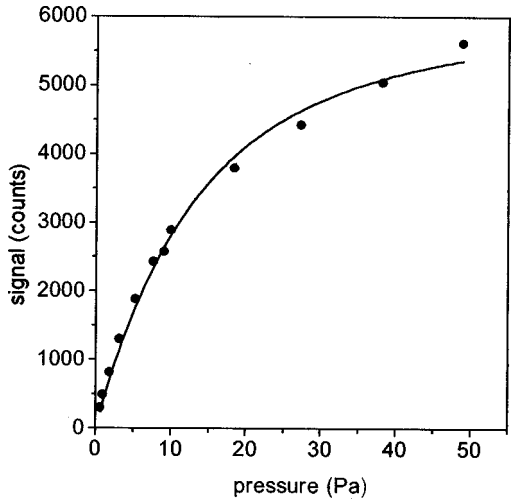

FIG. 3. Fluorescence signal from xenon after two-photon excitation as a function of pressure. The gate time is fixed at $T = 5$ μs. The solid line is a fit according to Eq. (3).

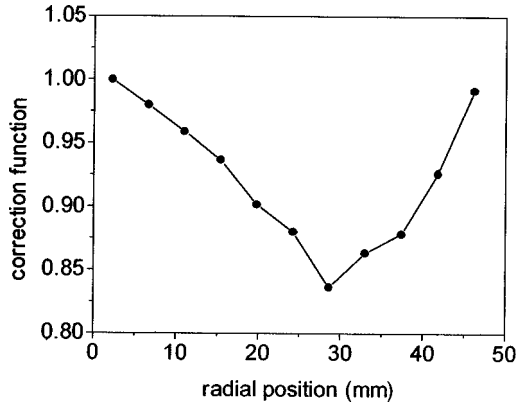

FIG. 4. Correction function for the radial density profile obtained from the xenon measurements.

$$S = B\, \frac{\alpha p}{1+\alpha p} \left[1 - \exp\left(-\frac{1+\alpha p}{1+\alpha p_0}\, \frac{t_g}{\tau_0}\right)\right] \tag{3}$$

with

$$\alpha = \frac{\tau k_Q}{k_B T_{\mathrm{Xe}}}. \tag{4}$$

From the fit the parameter α results: $\alpha = 0.101 \pm 0.008$ Pa^{-1}. This finally gives the lifetime $\tau = 5.0 \pm 0.6$ μs and the self-quenching rate coefficient $k_Q = 8.3 \times 10^{-11} \pm 1.6 \times 10^{-11}$ $\mathrm{cm}^3\,\mathrm{s}^{-1}$. These data could be used in a more detailed investigation to establish xenon as a reference gas for the absolute density calibration of atomic hydrogen. A similar application has been shown recently for xenon and atomic oxygen in Ref. 14.

Since the fluorescence wavelength in xenon is different from the hydrogen case there might be an error due to chromatic aberration. However, the resolution is much higher than the scale on which inhomogenities occur, and the changes due to chromatic aberration are so small that this error can be neglected (the calculated change in the magnification factor is only 0.7%). The spatial correction function obtained from these measurements is shown in Fig. 4. The uncorrected density values have to be multiplied by this factor in order to obtain the real values.

B. Absolute density calibration by a flow tube reactor

A flow tube reactor is connected to the discharge chamber in order to arrive at the absolute number density of hydrogen atoms.[15,16] A sketch of the flow tube reactor is shown in Fig. 5. Atomic hydrogen is generated in this reactor by dissociation in a microwave discharge. The discharge region is located outside the chamber, and a stream of helium and hydrogen is guided by a Teflon tube to the center of the electrode gap. The flow tube reactor is connected to a separate flange under 45° with respect to the laser beam and the entire setup for the discharge and the diagnostics remains unchanged. As shown in the lower part of Fig. 5 the generated atomic hydrogen density is constant only over the range of the main tube orifice and decreases linearly outside this region. Therefore the calibration measurements are per-

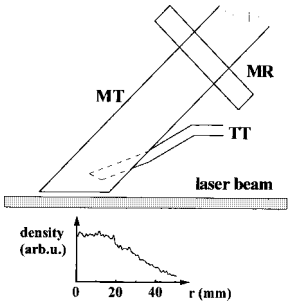

FIG. 5. Scheme of the flow tube reactor (MR: microwave resonator, MT: main tube, TT: titration tube). The relative atomic hydrogen density distribution along the laser beam is shown in the lower part of the figure.

formed only in the central region. As for the xenon measurements it was verified that the signal scales with the square of the laser intensity.

The absolute density is deduced in the following way from a titration measurement with NO_2: Through a second tube, the ''titration tube,'' a stream of helium and NO_2 is guided to a point close to the end of the main tube (about 2.5 cm distance). At the point where the two tubes intercept the gas flows are mixed. NO_2 reacts in this region with atomic hydrogen according to

$$NO_2+H\rightarrow NO+OH. \tag{5}$$

Atomic hydrogen is destroyed, and the fluorescence signal is now recorded as a function of the flux of NO_2. An additional amount of helium is added to the flux through the titration tube when the NO_2 flux is changed in order to keep the total flux constant. Since each NO_2 molecule destroys one hydrogen atom, the signal decreases linearly with the NO_2 flux. By linear extrapolation to zero signal one obtains the so called titration flux, ϕ_T, where the NO_2 flux equals the flux of atomic hydrogen. From this flux, the total gas flux ϕ_S, the pressure, and from the gas temperature, the atomic hydrogen density n_{H} results by the following relation

$$n_{\mathrm{H}}=\frac{p}{kT}\frac{\Phi_T}{\Phi_S}. \tag{6}$$

All fluxes are measured and controlled by flow meters and flow controllers. The absolute pressure is measured by a capacitive pressure gauge. NO_2 is diluted in helium and the exact concentration of 1.15% was verified immediately before the measurement by infrared absorption spectroscopy. The laser energy was monitored by a pyroelectric energy meter. The temperature of atomic hydrogen was determined as $T=300$ K by scanning the laser over the two-photon resonance and measuring the residual Doppler width. The overall precision of the calibration is estimated to be about 15%. Depending on the conditions (pressure, microwave power, fluxes) atomic hydrogen densities of the order of 10^{20} m^{-3} are generated. Typical conditions are $P=40$ W, $p=800$ Pa, $\Phi_S=1000$ sccm, $\Phi_{\mathrm{H2}}=2$ sccm, $\Phi_T=1$ sccm.

The calibration constant obtained for the center of the discharge is in our case 6.22×10^{18} m^{-3} s mJ^2 counts^{-1}. ''Counts'' is the signal unit of the ICCD camera, and the time unit refers to the integration time of the camera. If, e.g., 10^4 counts are measured with an integration time of 10 s (100 laser shots) and a laser energy of 3 mJ, a density of 6.9×10^{20} m^{-3} results. The calibration constant is also a measure for the detection limit. At an integration time of 30 s (300 laser shots) a signal amplitude of 100 counts minimum is necessary to discriminate reasonably against noise. This corresponds to an atomic hydrogen density of about 2×10^{12} m^{-3}.

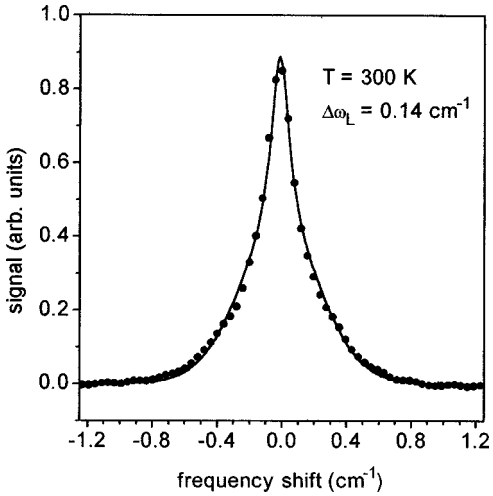

FIG. 6. Doppler-free two-photon excitation line profile in atomic hydrogen. The solid line is a fit based on the theoretical formula [Eq. (7)].

The measured densities in the rf discharge are corrected further for quenching of the excited atoms by collisions with hydrogen molecules. Quenching can be neglected in case of the measurements with the flow tube reactor since the molecular hydrogen densities are too small (of the order of 10^{20}–10^{21} m^{-3}) and helium is a very inefficient quencher. The quenching rate coefficients are taken from Refs. 17 and 18. Taking into account pulse-to-pulse fluctuations of the laser energy the overall error in the determination of the absolute densities in the rf discharge is estimated to be about $\pm15\%$.

IV. MEASUREMENTS IN THE rf DISCHARGE

A typical line profile in the rf discharge obtained with the laser wavelength scanned over the two-photon resonance is shown in Fig. 6. ''Typical'' means that this measurement has been repeated at various positions within the discharge and under various discharge conditions (power, pressure) with the same result. The solid line corresponds to a fit to a theoretical profile $g(\omega)$, where ω is the frequency of the laser at $\lambda=205$ nm. This profile is calculated by the standard formula[19] and convolution with the spectral profile of the laser. A Lorentzian spectral profile is assumed for the laser with a full width at half maximum of $\Delta\omega_L\ll\Delta\Omega_D$. The Doppler width at 300 K is $\Delta\Omega_D=1.2$ cm^{-1}. In addition, the measured transmission for a double pass through the chamber window for the back-reflected beam is included ($T=0.77$). Also the so-called ''photon-statistical factor''[20] of $G=2$ is taken into account for the Doppler-broadened contribution, and $G=1$ for the Doppler-free part.

$$g(\omega)=\exp\left[-4\ln(2)\left(\frac{\Omega-2\omega}{\Delta\Omega_D}\right)^2\right]+\frac{1}{\sqrt{4\pi\ln(2)}}\frac{T}{1+T^2}\times\frac{\Delta\Omega_D}{\Delta\omega_L}\frac{1}{1+\left(\frac{\Omega-2\omega}{\Delta\omega_L}\right)^2} \quad (7)$$

with

$$\Delta\Omega_D=\frac{\Omega}{c}\sqrt{\frac{8\ln(2)k_BT_{\rm H}}{m_{\rm H}}}. \quad (8)$$

Here, $\Omega=97\,492.3$ cm^{-1} is the two-photon transition frequency, c the speed of light, k_B the Boltzmann constant, $m_{\rm H}$ and $T_{\rm H}$ the mass and the temperature of the hydrogen atom, and ω the frequency of the laser radiation. The first part of Eq. (7) describes the Doppler-broadened background and the second part the Doppler-free excitation. The ratio of these two contributions is proportional on resonance to the ratio of the laser and the Doppler linewidths. The only fitting parameters, besides an amplitude factor, are the bandwidth of the laser and the Doppler width of the hydrogen atoms. The best fit is obtained for a laser bandwidth of $\Delta\omega_L=0.14$ cm^{-1} and a particle temperature of $T=300$ K with an uncertainty of about 5%.

The laser bandwidth and the spectral profile at the fundamental wavelength at $\lambda=615$ nm are measured by an etalon (finesse=50, free spectral range=0.333 cm^{-1}). The resulting Lorentzian profile has a bandwidth of 0.05 cm^{-1}. Consequently, about three times this value results after frequency tripling to $\lambda=205$ nm.

It should be noted that in similar discharges but without a showerhead electrode we find much higher temperatures—up to 1200 K. The main mechanism for the gas heating are probably charge exchange collisions in the sheath at the powered electrode. In our case fresh gas at ambient temperature is inserted at this position and cooling is therefore very efficient. In addition both electrodes are water cooled. One can conclude that the gas temperature within the discharge is strongly influenced by the gas exchange rate.

It should further be noted that in the general case where the gas temperatures in the calibration measurements and in the discharge are significantly different and only the signal amplitude at the resonance position is used for the determination of the particle density, the temperature ratio has to be taken into account as a correction factor for the Doppler-broadened background.

A contour plot of the absolute atomic hydrogen density distribution in the discharge is shown in Figs. 7(a) and 7(b). The pressure is 50 Pa and the discharge power is (a) 50 W and (b) 20 W, corresponding to a peak-to-peak voltage of 766 and 588 V, respectively. In order to emphasize variations in the density profile, the scales are different in Figs. 7(a) and 7(b), and the scales do not start at zero density. The hydrogen density is highest close the radial center of the discharge and close to the powered electrode. Atomic hydrogen diffuses from the discharge region between the electrodes towards the surrounding volume; therefore a density gradient builds up. The slight shift of the maximum off center is probably related to the influence of the grounded guard ring in the GEC cell. Spatial density profiles with a maximum off center have been reported in the GEC cell, e.g., for CF_2 densities in CF_4/Ar discharges[21] and for the electron density in Ar discharges.[22]

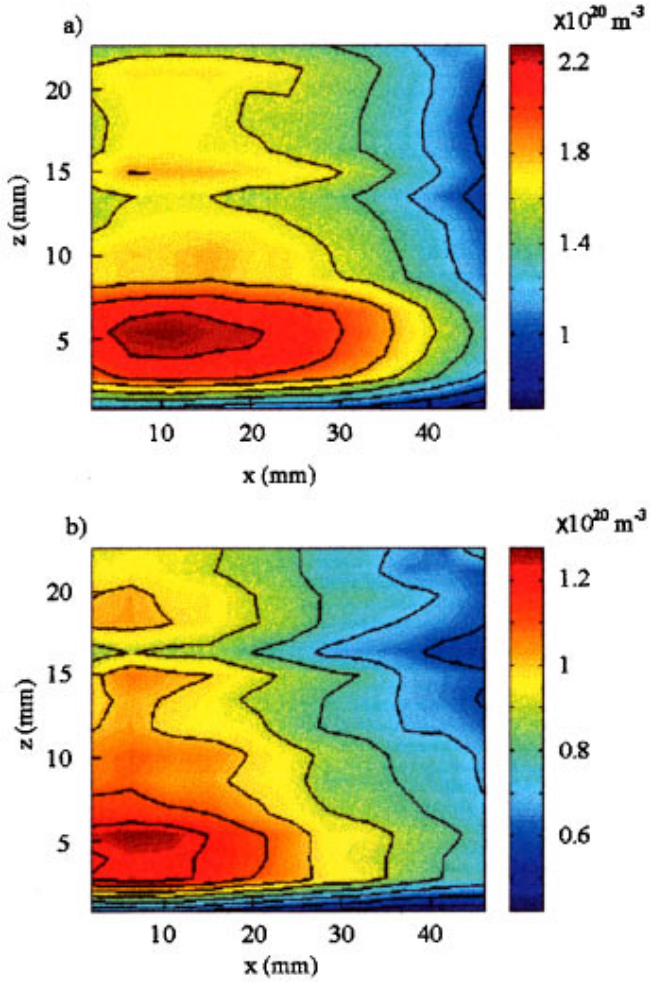

FIG. 7. Map of the absolute atomic hydrogen density within the discharge at $p=50$ Pa and at two different rf powers: (a) $P=50$ W, $U_{\rm pp}=766$ V, $U_B=300$ V, (b) $P=20$ W, $U_{\rm pp}=588$ V, $U_B=210$ V. The contour lines in the figure represent lines of constant density. x is the radial direction and z the vertical direction. The powered electrode is at $z=0$. Densities are represented by colors. A scale is given at the right side of the figures. It should be noted that in order to emphasize density fluctuations the scale does not start at zero.

The axial profile is also shown in Fig. 8. The plasma induced emission profile of the Balmer-α line is plotted in addition for comparison. In the axial direction the electrodes can ''shadow'' the plasma-induced emission collected by the detection optics. This can be corrected by a simple formula given in Ref. 23. The critical distance from the electrode where shadowing becomes effective is 1.2 mm. Therefore, only the data points at the edge are corrected.

The atomic hydrogen density peaks at a position between the two emission maxima. These emission maxima represent the double-sheath structure typical for hydrogen rf discharges.[24–26] The peak close to the electrode is related to field reversal during the period of positive applied voltage, and the peak further away is caused by the sheath expansion.

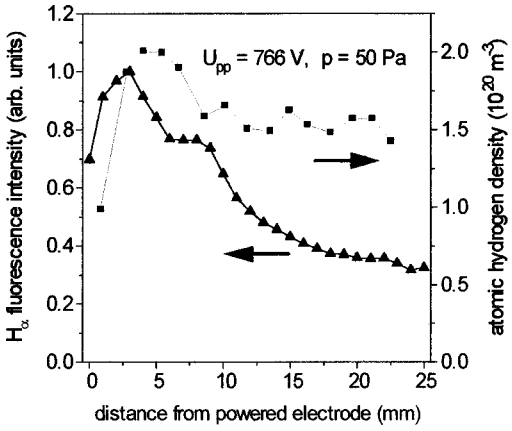

FIG. 8. Radial profile of the absolute atomic hydrogen density and the plasma-induced fluorescence emission at Balmer α at a pressure of $p=50$ Pa and a peak-to-peak voltage of $U_{pp}=766$ V.

In both phases energetic electrons are generated that cause excitation as well as dissociation. It is natural that the hydrogen density peaks in that region while it strongly decreases towards the electrodes due to surface recombination. The concave profile in the center is surprising, however. It cannot be explained by a simple one-dimensional diffusion model[27] without the assumption of a sink for hydrogen atoms in the center of the discharge. Since this is not very likely one might speculate on radial flow and diffusion effects which could be more pronounced in the center than close to the electodes. Further investigations are necessary to clarify this effect.

The dissociation degree in the center of the discharge depends linearly on the discharge pressure, if the peak-to-peak voltage is kept constant (Fig. 9). The bias voltage is not exactly constant with pressure but does not change more than by $\pm 5\%$. The bias voltages given in Fig. 9 are the average voltages. The linear rise indicates that the number of energetic electrons increases also. At the low pressure limit and at voltages above $U_{pp}=600$ V the dissociation degree rises again. This is probably due to the transition of the discharge from the so called ''alpha mode'' to the ''gamma mode,'' i.e., secondary electron emission from the electrode surface due to bombardment by energetic ions at low pressure and high voltage.[28] The dissociation degree varies between 1% and 5%, depending on pressure and voltage.

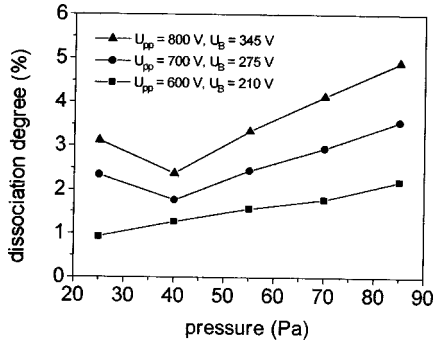

FIG. 9. Pressure dependence of the degree of dissociation at constant peak-to-peak voltages. The peak-to-peak voltages and the bias voltages are shown in the figure.

V. SUMMARY

Doppler-free excitation of atomic hydrogen in a rf discharge with narrow bandwidth radiation at $\lambda=205$ nm has been demonstrated. Due to the increase in the excitation efficiency an unfocused laser beam can be used. In combination with an ICCD camera this gives immediate information about the density profile along the laser beam. In order to correct for spatial inhomogenities in the excitation and the detection of the fluorescence light, two-photon excitation in xenon has been used as a reference. In connection with this calibration the exact value of the $15p[2\,1/2](j=2)$ Rydberg state in xenon and the natural lifetime and the self-quenching coefficient have been determined. The Doppler-free technique has been applied to the mapping of the absolute density in the discharge region of a rf discharge in pure hydrogen under various discharge conditions. The method is very sensitive with a detection limit of about 2×10^{18} m^{-3}.

Note added in proof: A nontrivial error has occurred in the determination of the NO_2 concentration in the NO_2/He mixture used for the titration measurement. The absolute NO_2 concentration was determined by Fourier transform infrared absorption spectroscopy. The absorption band at 1600 cm^{-1} used for analysis shows an unexpected large pressure broadening. We became aware of this influence only recently. The error in the measurement of the absolute NO_2 concentration caused by this line broadening effect is determined to be about 30%. All numbers for absolute atomic hydrogen densities and dissociation degrees have therefore to be multiplied by a factor of 1.3 in order to give the correct values.

ACKNOWLEDGMENTS

One of the authors (L.C.) would like to thank the Alexander von Humboldt Foundation for a postdoctoral grant. This work was supported by the Deutsche Forschungsgemeinschaft in the frame of the SFB 191 and by the Bundesminister für Bildung und Forschung (BMBF). Expert technical support by Rainer Führer is gratefully acknowledged. The authors also want to thank Michael Spaan for the determination of the NO_2 concentration.

[1] J. R. Roth, *Industrial Plasma Engineering* (Institute of Physics, London, 1995).
[2] B. Chapman, *Glow Discharge Processes* (Wiley, New York, 1980).
[3] IEEE Trans. Plasma Sci. **PS-14**, 2 (1986).
[4] Anon., *Plasma Processing of Materials: Scientific Opportunities and Technological Challenges* (National Academic, Washington DC, 1991).
[5] K. Nomoto, Y. Urano, J. L. Guizot, G. Ganguly, and A. Matsuda, Jpn. J. Appl. Phys., Part 2 **29**, L1372 (1990).
[6] D. P. Dowling, T. P. O'Brian, H. F. Döbele, V. Kornas, W. G. Graham, and R. Cheshire, Diamond Relat. Mater. **3**, 702 (1994).
[7] T. G. M. Freegarde and G. Hancock, J. Phys. IV, C4-15 (1997).
[8] U. Czarnetzki, J. Phys. IV **7**, C4-175 (1997).
[9] U. Czarnetzki, K. Miyazaki, T. Kajiwara, K. Muraoka, M. Maeda, and H. F. Döbele, J. Vac. Sci. Technol. A **12**, 831 (1994).
[10] J. E. M. Goldsmith and L. A. Rahn, Opt. Lett. **15**, 814 (1990).

[11] P. J. Hargis, K. E. Greenberg, P. A. Miller, J. B. Gerado, and J. R. Torczynski, Rev. Sci. Instrum. **65**, 140 (1994).
[12] M. A. Sobolewski, J. Res. Natl. Inst. Stand. Technol. **100**, 341 (1995).
[13] C. Moore, *Atomic Energy Levels* (Natl. Stand. Ref. Data Ser., Natl. Bur. Stand (U.S.), Washington, 1971), Vol. III.
[14] A. Goehlich, T. Kawetzki, and H. F. Döbele, J. Chem. Phys. **108**, 9362 (1998).
[15] D. W. Setser, *Reactive Intermediates in the Gas Phase* (Academic, New York, 1979).
[16] U. Meier, K. Kohse-Höinghaus, L. Schäfer, and C.-P. Klages, Appl. Opt. **29**, 4993 (1990).
[17] J. Bittner, K. Kohse-Höinghaus, U. Meier, and Th. Just, Chem. Phys. Lett. **143**, 571 (1988).
[18] B. L. Preppernau, K. Pearce, A. Tserepi, E. Wurzberg, and T. A. Miller, Chem. Phys. **196**, 371 (1995).
[19] W. Demtröder, *Laser Spectroscopy* (Springer, Heidelberg, 1981).
[20] R. Loudon, *The Quantum Theory of Light* (Clarendon, Oxford, 1973).
[21] B. K. McMillin and M. R. Zachariah, Proceedings of the 12th International Symposium on Plasma. Chem., Minneapolis, MN, 1995, Vol. 1, p. 539.
[22] M. B. Hopkins, Proceedings of Frontiers in Low Temperature Plasma Diagnostics II, Bad Honnef, 1997, p. 19.
[23] B. L. Preppernau and T. A. Miller in *Glow Discharge Spectroscopy*, edited by R. K. Marcus (Plenum, New York, 1993).
[24] F. Tochikubo, T. Makabe, S. Kakuta, and A. Suzuki, J. Appl. Phys. **71**,2143 (1992).
[25] M. M. Turner and M. B. Hopkins, Phys. Rev. Lett. **69**, 3511 (1992).
[26] C. M. O. Mahony, R. Al Wazzan, and W. G. Graham, Appl. Phys. Lett. **71**, 608 (1997).
[27] A. D. Tserepi, J. R. Dunlop, B. Preppernau, and T. A. Miller, J. Appl. Phys. **72**, 2638 (1992).
[28] S. M. Levitzky, Zh. Tekh. Fiz. **27**, 970 (1957).